5. (a) C. L. Hussey, in *Chemistry of Nonaqueous Solutions: Current Progress*, G. Mamantov and A. I. Popov, Editors, Chap. 4, VCH, New York (1994); (b) R. T. Carlin and J. S. Wilkes, *ibid.*, Chap. 5.
6. T. J. Melton, J. Joyce, J. T. Maloy, J. A. Boon, and J. S. Wilkes, *This Journal*, **137**, 3865 (1990).
7. C. L. Yu, J. Winnick, and P. A. Kohl, *ibid.*, **138**, 339 (1991).
8. J. Fuller, R. A. Osteryoung, and R. T. Carlin, *ibid.*, **142**, 3632 (1995).
9. G. E. Gray, P. A. Kohl, and J. Winnick, *ibid.*, **142**, 3636 (1995).
10. B. J. Piersma, D. M. Ryan, E. R. Schumacher, and T. L. Riechel, *ibid.*, **143**, 908 (1996).
11. M. A. M. Noel, P. C. Trulove, and R. A. Osteryoung, *Anal. Chem.*, **63**, 2892 (1991).
12. I-W. Sun, E. H. Ward, and C. L. Hussey, *Inorg. Chem.*, **26**, 4309 (1987).
13. I-W. Sun and C. L. Hussey, *ibid.*, **29**, 3670 (1990).
14. T. M. Laher and C. L. Hussey, *ibid.*, **21**, 4079 (1982).
15. C. L. Hussey and T. M. Laher, *ibid.*, **20**, 4201 (1981).
16. R. J. Gale, B. Gilbert, and R. A. Osteryoung, *ibid.*, **18**, 2723 (1979).
17. C. Nanjundiah and R. A. Osteryoung, *This Journal*, **130**, 1312 (1983).
18. A. J. Dent, K. R. Seddon, and T. Welton, *J. Chem. Soc., Chem. Commun.*, 315 (1990).
19. A. K. Abdul-Sada, A. M. Greenway, K. R. Seddon, and T. Welton, *Org. Mass Spectrom*, **24**, 648 (1992).
20. D. A. Nissen, *This Journal*, **126**, 176 (1979).
21. D. M. Bush, Sandia Laboratories, Albuquerque, NM, Technical Report SC-RR-69-497A (1972).
22. S. C. Levy and F. W. Reinhardt, *This Journal*, **122**, 200 (1975).
23. E. E. Marshall and L. F. Yntema, *J. Phys. Chem.*, **46**, 353 (1942).
24. C. L. Hussey, L. A. King, and J. K. Erbacher, *This Journal*, **125**, 561 (1978).
25. T. P. Moffat, *ibid.*, **141**, L115 (1994).
26. H. C. De Long and P. C. Trulove, in *Molten Salts*, R. T. Carlin, S. Deki, M. Matsunaga, D. S. Newman, J. R. Selman, and G. R. Stafford, Editors, PV 96-7, p. 276, The Electrochemical Society Proceedings Series, Pennington, NJ (1996).
27. T. B. Scheffler, Ph.D. Dissertation, University of Mississippi, University, MS (1984).
28. (a) D. M. Gruen and R. L. McBeth, *Pure Appl. Chem.*, **6**, 23 (1963); (b) G. Harrington and B. R. Sundheim, *Ann. N. Y. Acad. Sci.*, **79**, 950 (1960).
29. R. S. Nicholson and I. Shain, *Anal. Chem.*, **36**, 706 (1964).
30. S. K. D. Strubinger, I-W. Sun, W. E. Cleland, Jr., and C. L. Hussey, *Inorg. Chem.*, **29**, 993 (1990).
31. (a) H. Linga, Z. Stojek, and R. A. Osteryoung, *J. Am. Chem. Soc.*, **103**, 3754 (1981); (b) P. A. Barnard and C. L. Hussey, *This Journal*, **137**, 913 (1990).
32. T. B. Scheffler and C. L. Hussey, *Inorg. Chem.*, **23**, 1925 (1984).
33. G. P. Smith, in *Molten Salt Chemistry*, M. Blander, Editor, p. 451, John Wiley & Sons, New York (1964).
34. A. J. Bard and L. R. Faulkner, *Electrochemical Methods*, John Wiley & Sons, New York (1980).
35. W-J. Gau and I-W. Sun, *This Journal*, **143**, 170 (1996).
36. W-J. Gau and I-W. Sun, *ibid.*, **143**, 914 (1996).
37. C. L. Hussey, I-W. Sun, S. K. D. Strubinger, and P. A. Barnard, *This Journal*, **137**, 2515 (1990).

Relative Dielectric Constant Measurements in the Butyronitrile-Chloroethane System at Subambient Temperatures

Robin B. Michnick*,[a] Kevin G. Rhoads, and Donald R. Sadoway*

Department of Materials Science and Engineering, Massachusetts Institute of Technology, Cambridge, Massachusetts 02139-4307, USA

ABSTRACT

By means of electrochemical impedance spectroscopy, the relative dielectric constant was measured as a function of composition and temperature in the butyronitrile-chloroethane system from −35 to −105°C. A customized cell was designed by iterative optimization; the equivalent circuit was used to assess the impacts of the electrical properties of the sample, the limitations of the instrumentation, and the data reduction technique. To account for strong local ordering effects due to molecular association in these solutions, a new model, termed "extended Kirkwood-Onsager" (EKO), was developed. For solutions rich in chloroethane, structural features are inferred with this model.

Introduction

As part of a systematic study of the physical chemistry of butyronitrile (BN), chloroethane (CE), and their solutions, the relative dielectric constant was determined as a function of temperature and composition by electrochemical impedance spectroscopy (EIS). Growing awareness of the potential advantages of processing materials at subambient temperatures had stimulated interest in cryogenic electrochemistry.[20] This work was conducted within the framework of a search for liquids that can serve as low-temperature electrolytes for the electrochemical modulation of superconductivity in cuprate materials, such as $Ba_2YCu_3O_{7-\delta}$.[22]

The relative dielectric constant of BN has been studied by a number of authors[1-3] at and near room temperature. Values of the relative dielectric constant of CE as a function of temperature have been reported by two authors.[4,5] This work extends the temperature ranges of the relative dielectric constants for pure BN and CE and measures the dependence of the relative dielectric constant of the binary solutions as a function of temperature and composition.

In order to cope with the high specific impedances of these liquids while minimizing stray capacitance, a customized apparatus was designed. This paper describes the apparatus, reports the measured values of the relative dielectric constant as a function of temperature and solution composition, and interprets the results using a modification of the Kirkwood model.

Experimental

In the experience of the authors, it was found that optimal design of an experiment for EIS measurements derives from focusing on the electrical characteristics of the system and the relationships among cell design, experimental protocol, and data reduction (see Fig. 1). The complex interplay among these various factors is quantified by the equivalent circuit.

The equivalent circuit is a mathematical and physical model of the electrical behavior of an electrochemical system. There are three representations of the equivalent cir-

* Electrochemical Society Active Member.
[a] Present address: Dynamics Research Corporation, Wilmington, MA 01887, USA.

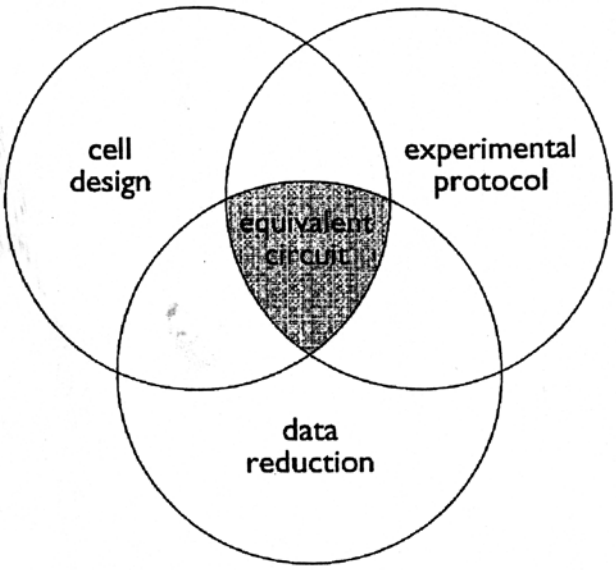

Fig. 1. Venn diagram showing relationships among factors in making electrical property measurements.

cuit: physical, graphical, and mathematical. A physical representation, a breadboard, is constructed of discrete circuit elements, *e.g.*, resistors, capacitors, inductors, diodes, delay lines, etc. A graphical representation is a circuit diagram consisting of idealized elements. A mathematical representation is a set of equations expressing the behaviors both of the network and of the idealized elements. The elements and their arrangement, the network, are chosen so as to mimic the anticipated electrical behavior of the electrochemical system. The choice of elements need not be restricted to passive linear lumped-parameter elements; nonlinear electrode kinetics and spatially distributed effects such as diffusion-controlled mass transport can be represented with subcircuits and distributed elements, *e.g.*, transmission lines and op-amp subcircuits. The test for equivalence is the comparison of the measured response of the electrochemical system to the response of the equivalent circuit under identical stimuli. The equivalent circuit in conjunction with the anticipated value of specific properties of the specimen is then used iteratively to design the experimental cell and protocols, to present the raw data in their most useful form, and to analyze the data. The value of using the equivalent circuit as a link among the different aspects of experimental measurement and interpretation can be found in the present investigation.

The objective of this study was to measure the relative dielectric constant of the BN-CE system. The measurement of intensive properties, *e.g.*, relative dielectric constant or resistivity, is accomplished by measuring the related extensive properties of a sample, *i.e.*, capacitance or resistance, respectively, where these are related by the geometry of the measuring cell. In its most basic form, a capacitance cell consists of a pair of electrodes immersed in the liquid under investigation. In this study, parallel-plate electrodes were chosen for the capacitance cell, and EIS was chosen as the fundamental measuring technique.

To conduct EIS measurements, an ac stimulus is applied to the electrodes over a range of frequencies, and the electrical response is measured. The stimulus can take the form of either a voltage, in which one measures the current response, or a current, in which one measures the voltage response. In this study, voltage excitation was used and its magnitude set at a value below the decomposition potential of the liquid. Under these conditions, the electrical behavior of the capacitance cell can be modeled by the equivalent circuit shown in Fig. 2. Note that the expected contributions of the lead wires have been included. The value of the relative dielectric constant is contained in the response of element, C_S, the solution capacitance; however, it is impossible to measure this alone. The measurement includes the contributions of all the elements of the equivalent circuit. By modifying the cell design, the experimental protocol, and/or the method of data reduction (the principle elements of Fig. 1), the electrical responses of the obstructing elements are minimized or eliminated and the electrical response of the desired element is enhanced. The following paragraphs describe how these approaches were applied.

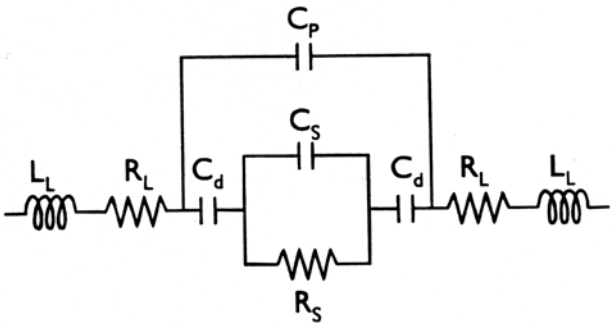

Fig. 2. Equivalent circuit of electrical property measurement.

Modifying cell design.—The magnitudes of R_L, the lead wire resistance, and L_L, the lead wire inductance, are minimized by using short lead wires, which has the added advantage of minimizing stray capacitance, C_P, arising from their interaction. C_P is also minimized by the use of coaxial cables for the segments of lead wire running from the instrument to the cell cap. By judicious choice of electrode geometry, the magnitude of C_S can be desirably increased (R_s is decreased simultaneously). Furthermore, in some cases one must consider also adjusting the values of C_S and R_s to ensure that they lie within the measuring range of the instrumentation. For the parallel plate electrodes used in this investigation, this is achieved by maximizing the ratio of electrode area to interelectrode gap.

Modifying cell design and experimental protocol.—Improving cell design can reduce R_L and L_L but it cannot eliminate their effects. In the cell used here, the impact of R_L on the total measured impedance is negligible over the frequency range used because the solutions under investigation are so resistive. In contrast, the impact of L_L needs to be further reduced, and this is achieved through modification of the experimental protocol. Hence, the wires running from the instrument to the cell cap are twisted together to reduce the area of the inductance loop, and the selected frequency range of the ac excitation voltage is chosen to reduce the magnitude of the associated impedance, *i.e.*, $j\omega L_L$. The frequencies required to measure C_S for the solutions under investigation are low enough that the impact of L_L can be made negligible.

Modifying experimental protocol.—The frequencies selected for the experiment also affect the magnitude of the impedance of the double-layer capacitance, $Z_{C_d} = 1/j\omega C_d$. In our cell, the value of C_d is estimated to be on the order of 100 μF, several orders of magnitude greater than C_S. In this investigation, over the range of frequencies required for the measurement of C_S, the impact of the C_d is negligible.

Modifying cell design, experimental protocol, and method of data reduction.—Shortening and separating the lead wires running from the cell cap to the electrodes minimizes C_P. Also, driven shields minimize the contributions to C_P from coaxial cables. Unfortunately, the measuring instrument used in this study, the Solartron Model 1260 frequency response analyzer, does not readily lend itself to operation with driven shields. Hence, magnetic reed switches were placed between the ends of the lead wires and the electrodes to allow measurement of C_P by controlled interruption of the electrical circuit. By making measurements with the switches in the open and closed

positions, the effect of C_P can be effectively eliminated during data analysis (see Fig. 3).

Final cell design.—The capacitance cell designed in the light of these considerations is shown in Fig. 4. The large ratio of electrode area to interelectrode gap was achieved by use of multiple, closely spaced, parallel-plate electrodes. Such an electrode structure is commercially available in the form of an air variable capacitor, (Hammarlund Model MAPC-75), in which the electrodes are made of nickel-plated brass. Both the large number and the close spacing of the electrode plates reduces the impact of the fringing fields. This is especially advantageous in eliminating sources of error derived from differences in electrical behavior between the calibration solution and the solution under investigation.

The BNC cables from the frequency response analyzer to the cell cap (E) were made as short as physically possible, 30 cm. The lead wires from the cell cap (E) to the electrode structure (H) were also made as short as possible, approximately 30 cm. Also shown in Fig. 4 are the two magnetic reed switches (I) mentioned previously.

The remainder of the cell is composed of an outer glass chamber topped with a stainless steel cap (E). The cap has five ports. The two electrode lead wires (A) were each sealed by epoxy into glass tubes which were fed through two of these ports. In order to be able to attach the cables from the measuring instrument reproducibly to the lead wires, notched copper fixtures (B) were soldered to their ends. Two ports accommodated closed-one-end glass tubes (C) which acted as guides for ALNICO™ magnets (G) that operated the magnetic reed switches (I). The last port, shown plugged in Fig. 4, accommodated a funnel used during charging of the cell. Through the use of compression fittings, the cell was rendered vacuum tight. Two valves (F) were welded to the cap for venting and vacuum drying the cell.

Solution preparation.—Prior to mixing, the two liquids were dried. BN was dried by successive application of drying agents. First, reagent grade liquid was poured onto a 3A molecular sieve and allowed to dehydrate for a minimum of 18 h. The liquid was then decanted and poured onto a new 3A sieve and again left for 18 h. This procedure was repeated twice more using activated alumina pellets as the desiccant. BN prepared in this manner exhibited an electrical conductivity of 1×10^{-8} S/cm at room temperature. This compares favorably with the value of 5×10^{-8} S/cm for BN prepared by distillation.[6] Clearly, the use of drying agents renders a liquid of superior purity, *i.e.*,

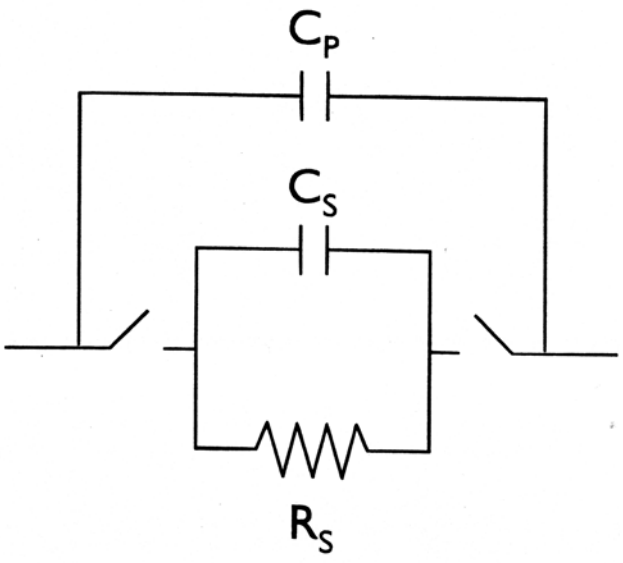

Fig. 3. Reduced equivalent circuit.

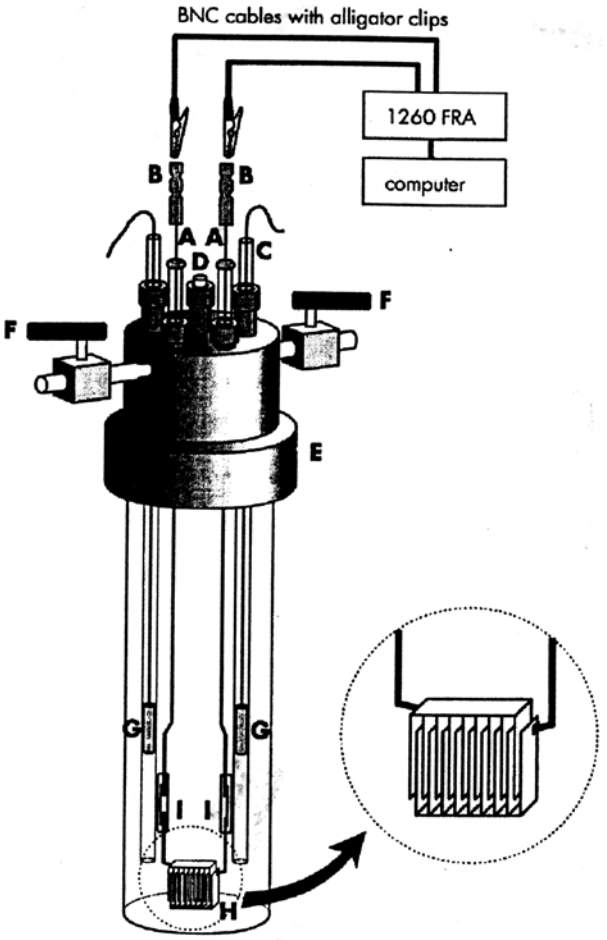

Fig. 4. Cell for measurement of electrical properties of highly resistive liquids.

lower residual water levels. CE was dried by condensing the gas on a 3A molecular sieve.

The compositions investigated were pure BN, 78.90 mole percent (m/o) BN, 56.91 m/o BN, 40.02 m/o BN, 18.35 m/o BN, and pure CE. The samples were measured by weight and mixed in a nitrogen-filled glove bag. Because CE is a gas at room temperature, the samples were kept cool in an external liquid nitrogen bath during mixing. Once mixed, the solutions were kept in sealed flasks at −30°C until use.

Protocol.—A typical experiment is conducted in the following manner. The capacitance cell is cleaned with distilled water and vacuum dried for at least 12 h. The cell, solution to be measured, and funnel are placed in a glove bag filled with dry nitrogen. To prevent drift in composition due to vaporization of CE, an external liquid nitrogen bath is used to cool the glove bag and its contents. Once in the dry nitrogen filled glove bag, one of the side valves (F) is opened and the Teflon® plug (D) is removed. The funnel is placed in this opening and the solution poured in. The plug is then replaced, and the valve shut. The cell is now removed from the glove bag and placed in the cryostat[7] the temperature of which has been set at a value of −35°C. Within 15 min thermal equilibrium is achieved.

The measurement begins with the lowering of magnets (G) to open the magnetic reed switches (I). Impedance is measured. The magnets are then raised and impedance measured three times. In data analysis, at each of many frequencies the differences are computed in the measured admittances with the switches open and closed and then inverted to give the impedances of the solution alone. The temperature is then lowered to the next set point value, and after a period of 15 min, the procedure is repeated. The temperature set points were −35°C (238 K), −50°C

(223 K), −65°C (208 K), −80°C (193 K), −95°C (178 K), and −105°C (168 K).

Calibration.—The cell was calibrated to determine the value of the cell constant, G. First an impedance measurement was made with the cell under vacuum. The capacitance of the cell was extracted from these data. The cell constant was computed by taking the measured capacitance of the cell divided by the known dielectric constant of vacuum. As a confirmation, the same procedure was repeated with methanol.[8-12] From both vacuum and methanol measurements made at different temperatures, it was demonstrated that G is invariant with temperature over the range of interest.

Instrumentation settings.—The instrumentation parameters were set by a personal computer using the Z60 impedance program (Scribner Associates, Inc., Charlottesville, VA). The frequency was set to vary logarithmically descending from 1 MHz to 500 Hz with 10 points per decade. The generator output was set for 300 mV with no bias. Voltage measurements were made on a 300 mV scale; current measurements were made on a 600 μA scale. Data were taken for a fixed integration time of 5 s following a three-cycle delay. In the special case of vacuum calibration the generator output was increased to 2.8 V, and the voltages were measured on the 3 V scale.

Data analysis.—At the conclusion of the experiment, the raw data consist of paired sets of measurements taken with the magnetic reed switches opened and closed. These data are treated by subtracting admittances, $Z^{-1}(\omega)$.

The values for the C_s and R_s were determined using a least squares fitting package, ZSIM (Scribner Associates, Inc., Charlottesville, VA) in conjunction with LEVM (J. Ross Macdonald, University of North Carolina, Chapel Hill, NC) to fit the data to the subcircuit located between the switches in Fig. 3. Typical measured and fit data are shown in Fig. 5 where the excellent agreement between model and measurement is clearly evident over an extremely wide range of frequency. The relative dielectric constant, ϵ_r, was computed from values of capacitance by the following relationship

$$\frac{C_{sample}}{C_{vacuum}} = \frac{\epsilon_o \epsilon_r G}{\epsilon_o G} = \epsilon_r \qquad [1]$$

where ϵ_o is the permittivity of free space and G is the value of the cell constant.

Results and Discussion

The values of ϵ_r computed from measurements are shown for pure BN in Fig. 6 and pure CE in Fig. 7. For BN no direct comparison is made with results reported in the literature. As can be seen in Fig. 6, the temperature range of this investigation was distinctly different from those of the other studies.[1-3]

For CE there is some discrepancy between the results of previous studies.[4,5] Although there is minimal overlap in temperature range, the temperature dependence observed in the present investigation more closely mirrors that of Nickerson and McIntosh.[5]

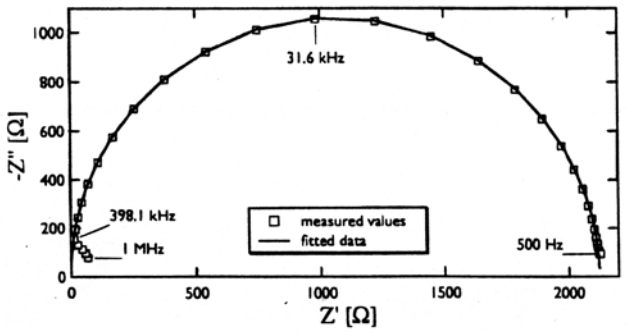

Fig. 5. Measured and modeled values of complex impedance of pure BN.

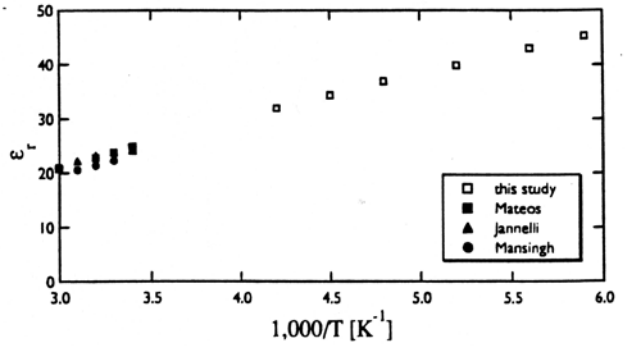

Fig. 6. Temperature dependence of the relative dielectric constant of pure BN.

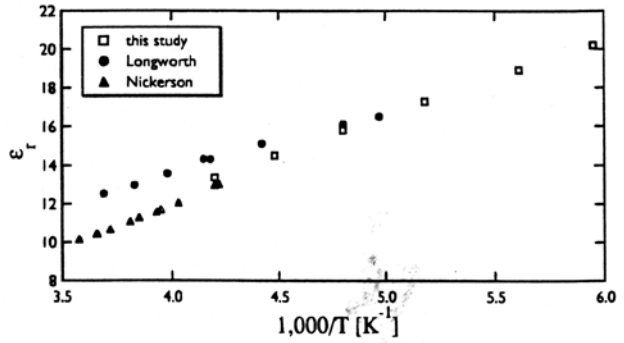

Fig. 7. Temperature dependence of the relative dielectric constant of pure CE.

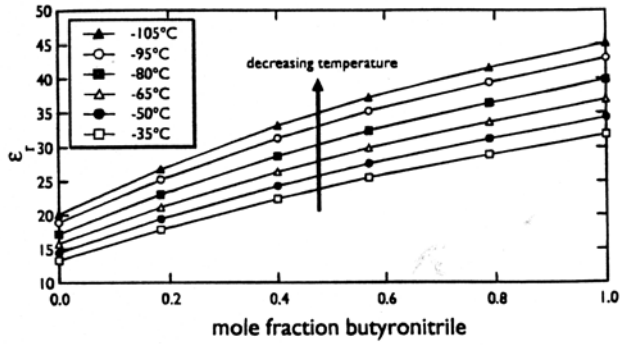

Fig. 8. Dependence of the relative dielectric constant on temperature and composition in the BN-CE System.

The variation of ϵ_r with composition and temperature is shown graphically in Figure 8 and is tabulated in Table I. The values of estimated total error are ±0.26 in ϵ_r, ±0.15°C in temperature, and ±0.05 m/o in composition.

As is the case with pure BN and CE, at constant composition ϵ_r of the binary solutions increases as temperature decreases. This behavior is consistent with the expected

Table I. Measured values of the relative dielectric constant.

Composition (m/o BN)	−35°C	−50°C	−65°C	−80°C	−95°C	−105°C
100.00	31.87	34.33	36.98	39.85	43.02	45.17
78.90	28.94	31.23	33.71	36.44	39.48	41.64
56.91	25.54	27.61	29.89	32.42	35.25	37.25
40.02	22.38	24.30	26.39	28.68	31.30	33.14
18.35	17.86	19.42	21.13	23.03	25.21	26.77
0.00	13.33	14.51	15.80	17.25	18.91	20.13

changes in density and thermal energy. The isothermal variation with concentration is nearly linear with a similar curvature at all temperatures measured. The deviation from ideal mixing can be expressed in terms of the excess relative dielectric constant, ϵ_r^{xs}, defined as

$$\epsilon_r^{xs} = \epsilon_{r,measured} - x_{BN}\epsilon_{BN} - x_{CE}\epsilon_{CE} \quad [2]$$

where x is the mole fraction. The isothermal variation of ϵ_r^{xs} with composition is shown in Fig. 9. Positive values of ϵ_r^{xs} show that the dipoles in solution align to give a greater net moment than that predicted by ideal mixing.[13-15] As temperature decreases, the magnitude of the maximum of the isotherm increases. The maxima of all the curves lie near 50 m/o BN. In the following section a modified Kirkwood model is presented in order to support the interpretation of these results.

Extended Kirkwood-Onsager model.—The relationship between atomistic properties of molecular species and the continuum properties of the bulk material can be viewed as a combination of several effects. Without accounting for local ordering, Onsager relates local molecular-level electric fields to continuum macroscale electric fields. Kirkwood accounts for local ordering under the assumption that all local ordering is diffuse, *i.e.*, the Onsager-computed dipoles remain unchanged. When there is molecular association (as is the case with solutions of BN and CE), the dipole moments of the associated species will clearly be different from those of free (unassociated) species. This manifests itself as another form of local ordering: strong, not diffuse. In the present investigation a new model, termed "extended Kirkwood-Onsager" (EKO), was developed to account for strong local ordering effects due to molecular association. The interpretation of the dielectric behavior of associated solutions requires the use of all these models in combination.

The temperature dependence of ϵ_r can be expressed by the Kirkwood equation,[16] written here in SI units

$$\frac{(\epsilon_r - 1)(2\epsilon_r + 1)}{3\epsilon_r} = \frac{N}{V\epsilon_o}\left(\alpha + \frac{g\mu^2}{3kT}\right) \quad [3]$$

where μ is the molecular dipole moment in the liquid, g is the Kirkwood correlation factor, α is the polarizability (a measure of the distortion polarizations, electronic and atomic), N is the Avogadro constant, k is the Boltzman constant, T is absolute temperature, and V is the molar volume. Kirkwood accounts for local ordering about each dipole through the correlation factor, g, under the assumption that the values of the dipole moments for the various species remain unchanged. In the presence of molecular association, the values of the dipole moments cannot be assumed invariant; in this case the Kirkwood equation allows determination of only the cumulative effect of all ordering, embedded in the quantity, $g\mu^2$.

In the absence of molecular association the value of μ can be computed by the Onsager relationship[17]

$$\mu = \frac{(2\epsilon_r + 1)(n^2 + 2)}{3(2\epsilon_r + n^2)}\mu_g \quad [4]$$

where n is the refractive index (typically the value at the sodium doublet multiplied by 1.1 where the additional 10% accounts for the atomic polarization effects) and μ_g is the value of the dipole moment as measured in the gas. The value of the correlation factor, g, determined under these conditions is a measure of diffuse local order in the liquid. However, when association occurs the attendant strong, local ordering is reflected in the value of μ. This is in addition to any diffuse, local ordering which is reflected in the value of g. In this case, the value of μ cannot be computed by Eq. 4 alone. Hence, in this investigation $g\mu^2$ was found for BN-CE solutions solely from Eq. 3 using values of ϵ_r measured at different temperatures. For pure BN and pure CE, the temperature dependence of the molar volume was calculated by the correlation

$$\rho = \frac{A}{B^{1+[1-(T/C)]^D}} \quad [5]$$

where ρ is density, T is temperature, and A, B, C, and D are coefficients whose values were determined by regression of selected values in the literature and are reported in Daubert and Danner.[18] Values of refractive index, n, were obtained by linear extrapolation of values reported at room temperature.[21] Values of the dipole moment as measured in the gas, μ_g, were taken from Daubert and Danner.[18] For binary solutions of BN-CE, there are no data for the variation in molar volume with composition and temperature; accordingly, the temperature dependence of the molar volume was calculated from the weighted, mole-fraction average of the pure components. As a consequence, in this analysis all effects due to deviations from ideal mixing in these solutions are assigned to the $g\mu^2$ term. The results are reported in Table II. Finally, diffuse and strong local ordering effects were separated by a method representing an extension of the Kirkwood model, a description of which follows.

Most generally, for a multicomponent solution, the value of $g\mu^2$ can be expressed in terms of the sum

$$g\mu^2 = \sum_i x_i\mu_i\mu_{env} \quad [6]$$

where Σ_i is evaluated over each molecular species present in the solution, x_i represents the mole fraction of i, μ_i is its dipole moment, and μ_{env} represents the net dipole moment of the environment acting on species i. This last quantity is given by

$$\mu_{env} = \sum_i x_i\mu_i g_i \quad [7]$$

where g_i is the correlation factor of i.

In the binary system, BN-CE, the following two assumptions were made about speciation. First, BN and CE react to form the 1:1 complex, BNCE, according to the equation

$$BN + CE \rightarrow BNCE \quad [8]$$

It is further assumed that this reaction goes to completion; hence, the mole number of BNCE can be calculated from simple stoichiometry. There is ample evidence of strong association in these solutions. For example, the measured phase diagram has a deep eutectic trough, and the shape

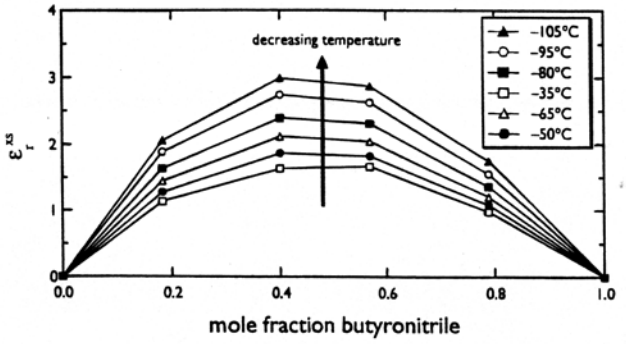

Fig. 9. Dependence of the excess relative dielectric constant on temperature and composition in the BN-CE system.

Table II. Values of $g\mu^2$ determined by the Kirkwood equation.

x_{BN}	$g\mu^2$ (Cm)^2
1.00	9.58×10^{-59}
0.79	8.68×10^{-59}
0.57	7.62×10^{-59}
0.40	6.73×10^{-59}
0.18	5.32×10^{-59}
0.00	3.89×10^{-59}

of the liquidus can be modeled as an associated solution containing 1:1 stoichiometric complexes.[19] Furthermore, it is assumed that BNCE and unreacted CE mix ideally, an assumption that is also supported by the results of thermodynamic modeling.[19]

Second, pure BN is known to form the bimolecular species $(BN)_2$, according to

$$2BN = (BN)_2 \quad [9]$$

In contrast to the reaction in Eq. 8, the reaction to form so-called $(BN)_2$ self-associates is assumed not to go to completion. The relative amounts of BN and $(BN)_2$ are given by

$$K = a_{(BN)_2}/a_{BN}^2 \quad [10]$$

The experimental results are interpreted within this framework and are summarized in Table III. Consider first CE-rich solutions which, according to the two assumptions, should consist of BNCE and CE. Under these circumstances, Eq. 6 is written as

$$g\mu^2 = x_{CE}\mu_{CE}\mu_{env} + x_{BNCE}\mu_{BNCE}\mu_{env} \quad [11]$$

where x_{CE} and x_{BNCE} represent the mole fractions of CE and BNCE, respectively, following the reaction between BN and CE according to Eq. 8, and μ_{env} is given by

$$\mu_{env} = x_{CE}\mu_{CE}g_{CE} + x_{BNCE}\mu_{BNCE}g_{BNCE} \quad [12]$$

For pure CE, in which there is no evidence of molecular association, the value of μ_{CE} can be calculated by Eq. 4 using data for pure CE. From this, g_{CE} can be determined from the value of $g\mu^2$ measured in this study. The resulting value of $g = 0.83$ is slightly less than unity, and thus suggests a net antiparallel alignment of the molecules, although the effect is expected to be small.

For CE-rich solutions, one can use the measured values of $g\mu^2$ at $x_{BN} = 0.40$ and 0.18 in order to estimate values of $\mu_{BNCE} = 2.33 \times 10^{-29}$ Cm and $g_{BNCE} = 0.121$. The computed value $\mu_{BNCE} = 2.33 \times 10^{-29}$ Cm is greater than the sum of the dipole moments of its two molecular components, BN and CE. Thus, it should not be surprising that there is significant antiparallel alignment around the BNCE complex. In the absence of ferroelectric poling effects, it is energetically favorable for dipoles located equatorially about a dipole to align antiparallel, while those located polarly align parallel. Since the total volume of the species, to any arbitrary radius, partitions unequally with the larger fraction contained in the equatorial regions, the expected environmental dipole moment is aligned antiparallel. Furthermore, this effect is expected to increase with increasing strength of the central dipole, since, among other reasons, the orientation energy will be large in comparison to kT. To go beyond this purely qualitative explanation requires a serious molecular-dynamics modeling effort, something well beyond the scope of this study. However, it is the opinion of the authors that such a modeling effort here is warranted and quite feasible, as the relevant volume about a dipole will be small and the number of molecules therein tractably few.

For BN-rich solutions, the speciation is more complicated owing to self-association of BN. Figure 9 reveals the lack of asymmetry in the compositional variation of ϵ_r^{xs}, *i.e.*, the shape of the isotherm is invariant with temperature over the entire temperature range of this investigation. If it is assumed that the dielectric behaviors of BN and $(BN)_2$ are distinguishable, then either self-association in BN is invariant with temperature or the extent of self-association must be extreme at all temperatures, *i.e.*, either very small or very large. Otherwise, at high BN concentrations one would expect deviation from simple parabolic in the shape of the isotherms. However, phase diagram measurements made in this laboratory of the BN-CE system reveal symmetry in the liquidus on either side of the deep eutectic trough centered at $x_{BN} = 0.50$, the composition of the BNCE complex.[19] This would tend to reject the possibility that $(BN)_2$ is the dominant species in BN-rich solutions. Thus, in the absence of information about the structure of $(BN)_2$ (to enable the determination of $\mu_{(BN)_2}$) or about the distribution of BN and $(BN)_2$ (the values of $x_{(BN)_2}$ and x_{BN} at equilibrium), further analysis of BN-rich solutions gives indeterminate results.

Table III. Summary of electrical properties of BN-CE binary solutions.

	μ (Cm)	g
CE [a]	0.68×10^{-29}	0.83
BNCE [b]	2.33×10^{-29}	0.12
BN [c]	1.36×10^{-29}	Indeterminate
$(BN)_2$	Indeterminate	Indeterminate

[a] These values were determined by the Onsager and Kirkwood models, respectively, using gas-phase data and dielectric measurements made on pure CE.

[b] These values were determined by the EKO model using dielectric measurements made on CE-rich solutions.

[c] This value was determined by the Onsager model using gas-phase data for pure BN with the assumption that self-association is negligible.

Conclusions

While relative dielectric constant measurements are not the obvious method with which to study liquid structure, this investigation has shown that in multicomponent solutions such data can be interpreted with the aid of an extended Kirkwood-Onsager model to provide insights into local properties of the molecular constituents. The EKO model offered herein can be applied to a wide variety of solutions, including those in which there is a strong degree of molecular association.

Acknowledgments

The authors wish to acknowledge the assistance of the following people and agencies for their contributions to this work: Professor Robert M. Rose for helpful discussions and for providing release time for Dr. Kevin G. Rhoads; Guenther Arndt for constructing the experimental apparatus; Dr. Naomi A. Fried, Dr. Kwang Bum Kim, Dr. Susan L. Schiefelbein, and Dr. Heather B. Shapiro for their helpful advice on making impedance measurements; the Office for Naval Research, the Strategic Defense Initiative Office (SDIO), and American Research and Development, Incorporated, for partial financial support.

Manuscript submitted Aug. 30, 1996; revised manuscript received March 21, 1997.

Massachusetts Institute of Technology assisted in meeting the publication costs of this article.

REFERENCES

1. L. Jannelli, A. Lopez, and L. Silvestri, *J. Chem. Eng. Data.*, **28**, 166 (1983).
2. M. C. Mateos, P. Perez, F. M. Royo, M. Gracia, and C. Gutierrez Losa, *Rev. Acad. Cienc. Exactas, Fis., Quim. Nat. Zaragoza*, **41**, 73 (1986).
3. K. Mansingh and A. Mansingh, *J. Chem. Phys.*, **41**, 827 (1964).
4. W. R. Longworth and P. H. Plesch, *J. Chem. Soc.*, 1618 (1959).
5. J. D. Nickerson and R. McIntosh, *Can. J. Chem.*, **35**, 1325 (1957).
6. A. D'Aprano and R. M. Fuoss, *J. Solution Chem.*, **3**, 1, 45 (1974).
7. H. B. Shapiro, Ph.D. Thesis, Department of Materials Science and Engineering, Massachusetts Institute of Technology, Cambridge, MA (1993).
8. C. S. Leung and E. Grunwald, *J. Phys. Chem.*, **74**, 696 (1970).
9. M. Nicolas, M. Malineau, and R. Reich, *Phys. Chem. Liq.*, **10**, 11 (1980).
10. F. Travers and P. Douzou, *J. Phys. Chem.*, **74**, 2243 (1970).
11. D. W. Davidson, *Can. J. Chem.*, **35**, 458 (1957).
12. D. J. Denney and R. H. Cole, *J. Chem. Phys.*, **23**, 1767 (1955).

13. L. Marcheselli, G. Pistoni, M. Tagliazucchi, L. Tassi, and G. Tosi, *J. Chem. Eng. Data*, **38**, 204 (1993).
14. J. Nath and M. Tevari, *J. Chem. Soc. Faraday Trans.*, **88**, 2197 (1992).
15. G. E. Papanastasiou and I. I. Ziogas, *J. Chem. Eng. Data*, **37**, 167 (1992).
16. J. G. Kirkwood, *J. Chem. Phys.*, **7**, 911 (1939).
17. L. Onsager, *J. Am. Chem. Soc.*, **58**, 1486 (1936).
18. T. E. Daubert and R. P. Danner, *Physical and Thermodynamic Properties of Pure Chemicals: Data Compilation*, Taylor and Francis, Washington, DC (1989).
19. R. B. Michnick and D. R. Sadoway, *J. Phys. Chem.*, **100**, 19628 (1996).
20. D. R. Sadoway, in *New Trends and Approaches in Electrochemical Technology*, N. Masuko, T. Osaka, and Y. Fukunaka, Editors, pp. 65-74, Kodansha, Ltd., Tokyo (1993).
21. J. A. Riddick, W. B. Bunger, and T. K. Sakano, *Organic Solvents*, 4th ed., John Wiley & Sons, Inc., New York (1986).
22. D. R. Sadoway and R. M. Rose, U.S. Pat. No. 4,911,800 (1990).